Immobilized proteins in buffer imaged at molecular resolution by atomic force microscopy

A. L. Weisenhorn, B. Drake, C. B. Prater, S. A. C. Gould, P. K. Hansma, F. Ohnesorge, M. Egger, S.-P. Heyn, and H. E. Gaub

Department of Physics, University of California at Santa Barbara, Santa Barbara, California 93106 USA; and Physik Department, Technische Universität Müchen, D-8046 Garching FRG

ABSTRACT Samples of supported planar lipid-protein membranes and actin filaments on mica were imaged by atomic force microscopy (AFM). The samples were fully submerged in buffer at room temperature during imaging. Individual proteins bound to the reconstituted membrane were distinguishable; some structural details could be resolved. Also, surface-induced, self-assembling of actin filaments on mica could be observed. Monomeric subunits were imaged on individual actin filaments. The filaments could be manipulated on or removed from the surface by the tip of the AFM. The process of the decoupling of the filamentous network from the surface upon changing the ionic conditions was imaged in real time.

INTRODUCTION

In recent years scanning probe microscopes have imaged surface structures down to an atomic level (1–3). The possibility of nondestructively imaging native, neither stained nor decorated, surfaces opens applications in functional as well as structural investigations of biologically relevant macromolecules (4). This paper (*a*) shows that individual proteins and protein complexes can be imaged with atomic force microscopy (AFM) down to a resolution where even molecular details are visible under physiological conditions of ionic strength and (*b*) demonstrates the experimental boundary conditions within which nondestructive imaging of proteins is possible now.

MATERIALS AND METHODS

Fab lipid

A proteolipid consisting of the antigen-binding fragment of a monoclonal antibody and a phospholipid was synthesized. In the following it will be referred to as Fab lipid. The details of the preparation are given elsewhere (Egger et al., manuscript submitted for publication). Briefly, Fab'2 fragments of the monoclonal anti DNP antibody AN02 (6), prepared by standard methods, were selectively cleaved into monovalent Fab' fragments by reduction with 20 mM dithiotreitol (DTT) at pH 4.5. The freshly reduced Fab' fragments were immediately brought into contact with lipid vesicles, prepared by ultrasonication, containing the synthesized *N*-[4-maleimido]-benzoyl-DPPE spacerlipid. The coupling reaction was performed for 6 h at 23°C. The conjugated proteolipid vesicles were finally separated from unbound material by density gradient centrifugation on metrizamide. The antigen-binding activity was confirmed to be retained when reconstituted in a supported membrane (7). All chemicals were purchased from Sigma Chemical Co. (St. Louis, MO) unless otherwise indicated.

Address correspondence to Dr. H. E. Gaub.

Supported planar membranes

A detailed description of the generation of supported planar membranes from vesicles is given elsewhere (8). Briefly, a monolayer was allowed to form at the air-water interface of the Fab lipid vesicle suspension and separated from adherent vesicles. The isolated monolayer was compressed in a home-built Langmuir trough (Heyn et al. manuscript submitted for publication) to 30 mN/m and transferred by horizontal dipping onto a silanized quartz slide. The whole process was controlled by fluorescence microscopy. Silanization of quartz slide with octadecyltrichlorosilane (OTS) was carried out as given in reference 10. The contact angle of a progressing drop of water was measured to be 105°.

Actin

Freshly purified actin was a kind gift of M. Bärmann. Details of the isolation and purification are given elsewhere (11, 12). After sterile filtration monomeric actin was stored in G-buffer (2 mM Tris-Cl [pH 7.5], 0.2 mM $CaCl_2$, 0.5 mM DDT, and 0.2 mM adenosine 5'-triphosphate [ATP]) on ice. The actin concentration was determined by UV absorption at 290 nm (specific absorption: 0.65 cm^2/mg). At a concentration <1mg/ml, actin is known to stay in its monomeric state in G-buffer (11). All experiments have been carried out within 1 wk after isolation. The samples were diluted in G-buffer just before imaging.

Experimental setup

Our AFM has been described in detail in previous publications (3, 13–15). A diamond tip attached to a microfabricated Si_3N_4 cantilever (16) was used to scan the sample surface. The cantilever is 100-μm long and has a spring constant of 0.9 N/m. Its deflection (when scanning the sample surface) is measured by the deflection of a laser light beam reflected off the back of the cantilever. Nanoscope feedback electronics and software are used to keep this deflection constant (Digital Instruments Inc., Santa Barbara, CA).

0006-3495/90/11/1251/08 $2.00

RESULTS AND DISCUSSION

One of the major advantages of AFM is its ability to image nonconducting samples in real time under physiological conditions of ionic strength and temperature making this technique ideally suited for imaging biological samples. One major problem, however, is that these samples are generally soft and flexible. Therefore the molecules of interest must be immobilized at a solid substrate. In our two cases this immobilization was done either by chemically linking the molecule to a supported lipid membrane or by electrostatic adhesion to the substrate combined with lateral polymerization.

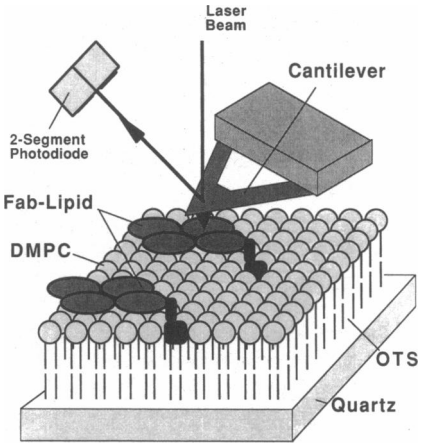

FIGURE 1 In this schematic diagram of our AFM, laser light is focused on a cantilever which reflects it toward a two-segment photodiode. The photodiode senses the deflection of the cantilever by sensing the position of the reflected beam. In operation, a feedback loop keeps the position of the reflected beam and hence the force on the sample constant. Also shown is a greatly magnified sketch of the type of sample that gave the images in Fig. 2.

Membrane-bound protein

Most communicative processes that are relevant for the function of cells occur at their plasma membrane. Therefore the investigation of these membranes is of greatest importance. Unfortunately, these membranes are two-dimensional fluids. A native cell membrane will thus not be rigid enough for molecular resolution when imaged with the AFM. However, several techniques have been developed in recent years to reconstitute and immobilize protein-containing lipid membranes on solid supports (17). Such systems have already been useful models for the investigation of certain processes occurring on cell membranes like molecular recognition (18). To study the latter set of problems we have recently developed a suitably designed lipid anchored receptor based on the antigen-binding fragment (Fab) of a monoclonal antibody covalently linked to a phospholipid (5). For the experiments reported here a monolayer of these molecules together with excess phospholipid was allowed to form at the air-water interface. The film was then compressed and driven into a two-dimensional phase segregation resulting in a protein rich phase embedded in an essentially pure lipid phase. This film was then transferred by vertical dipping onto an alkylated quartz slide resulting in an asymmetric membrane with the lower monolayer being chemically bound to the substrate.

Fig. 1 shows schematically the experimental setup used for imaging and, grossly exaggerated in size, the molecular model of such a supported membrane containing our Fab lipids. Fig. 2 *a* is an image of the membrane at low magnification. At low applied force (<5 nN) longish elevated surface structures were visible. The surface structures were predominantly oriented perpendicular to the fast scan direction. The image was stable for several minutes of scanning. Only in areas where the proteins were so dense that they were jammed into each other as in Fig. 2 *a*, submolecular details were visible. In this case four-leaved structures $\sim 12 \times 6 \times 2$ nm^3 ($\pm 15\%$) in size were observed (at about one-third of image size from the right edge and one-third from the bottom). On areas where the proteins were sparse, no submolecular structure was resolved and the proteins appeared as blobs. Under the same conditions no such surface structures could be seen on a pure lipid membrane. It is well known that antibodies are structured in domains (19) which have a characteristic pattern of crossed beta-pleated sheets, a structural feature which is conserved in a variety of receptor molecules. This evolutionarily stable motive might be reflected in the mechanical stability of the molecule, too. It is therefore very likely that the four leaves in Fig. 2 *a* represent individual immunoglobulin domains of the Fab fragment. The apparent size of this structure is ~30% bigger than expected. This is most likely due to the fact that the image is a nonlinear convolution of the real surface with the tip which leads to an increase of the appearent lateral dimensions depending on the tip shape (20). It is also possible that mechanical deformations due to the tip/sample interaction lead to a distortion of the image.

At a higher magnification and at somewhat higher forces (on the order of 10^{-8} N) the surface at the same position showed a texture where row-like protrusions with an average distance of ~0.4–0.5 nm were the dominant pattern (Fig. 2 *b*). Under equivalent conditions the same pattern could also be observed on a pure lipid membrane. This pattern was stable for several minutes of scanning but it disappeared upon increasing the force above 50 nN. We know from lateral diffusion measurements (21) that the lipids in this membrane are virtually immobile and in

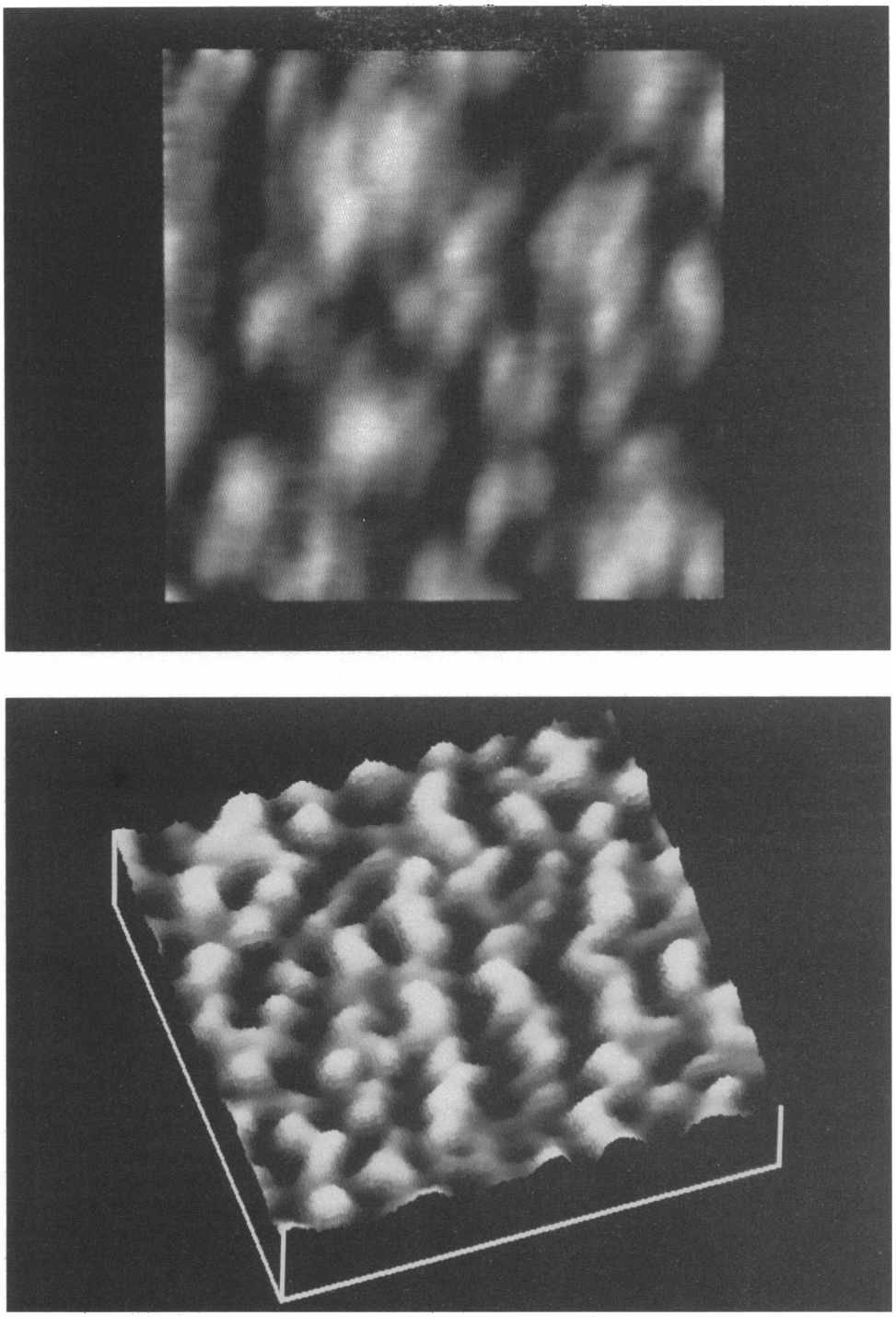

FIGURE 2 AFM images of Fab fragments on a planar membrane. Quartz was used as substrate to support the membrane. The images were taken at room temperature with the membrane submerged in Hepes buffer. (*a*) This image was recorded at low magnification showing the protein moiety of the mixed membrane. The surface is crowded with structures which seem to be jammed into each other. The predominant motive is the four-leaved structure outlined. Note that this surface structure was measured only at forces smaller than 5 nN (image size: 39.9 nm, height: ~2 nm). (*b*) This image was recorded at a high magnification in the same area as above at a scanning force of 10 nN. The image was stable over minutes besides of a slow lateral drift of the entire image (image size: 2.4 nm).

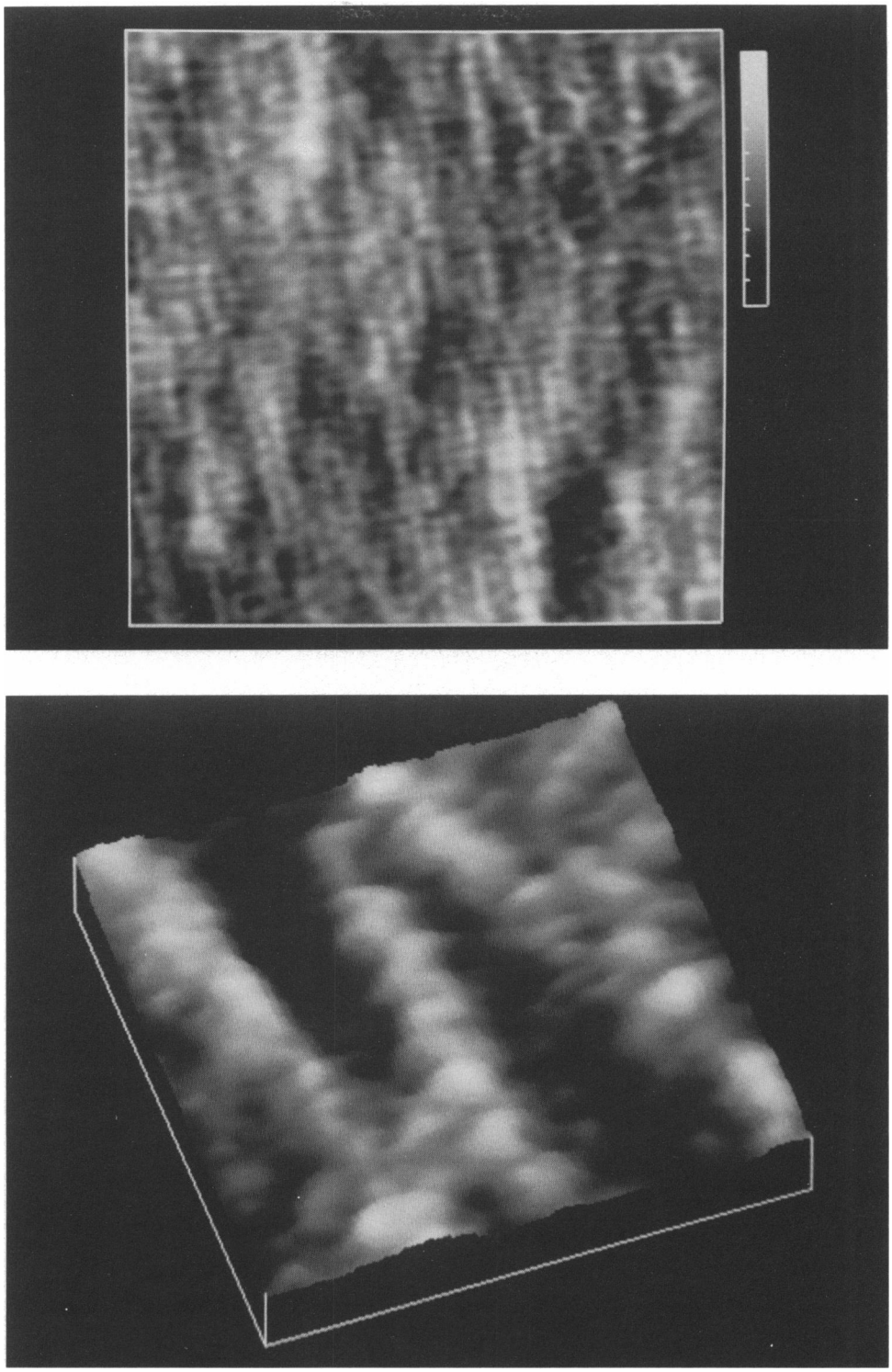

FIGURE 3 Images of actin filaments formed on the surface of freshly cleaved mica by surface-induced polymerization. (*a*) This AFM image was followed to appear after the mica surface was incubated with G-buffer containing monomeric actin. The filaments formed on the surface within <5 min. The force was always kept below 5 nN (image size: 454.5 nm, height: ~3.0 nm). (*b*) Same area as above but seen at a much higher magnification showing an individual filament. Again the force was always kept below 5 nN (image size: 60.7 nm, height ~0.2 nm).

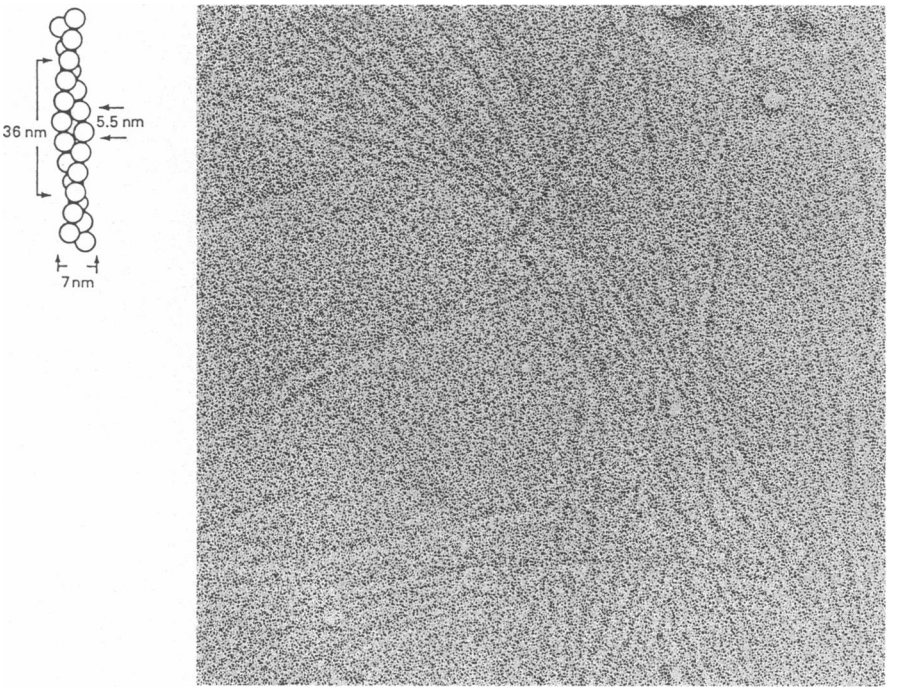

FIGURE 3 (*c*) Schematics of an actin filament assembled from its globulary subunits. Taken from reference 26. (*d*) TEM-image of actin filaments on mica (image size: 100 nm). Actin was allowed to self-assemble on the freshly cleaved mica surface for 15 min. The sample was then rinsed with deionized water, dried, and a platinum decorated carbon replica was made. For details see reference 29.

a solid phase. The predominant periodicity in such a membrane is on the order of 0.4–0.5 nm, depending on the tilt of the tightly packed hydrocarbon chains. It seems therefore very likely that the surface structure shown in Fig. 2 *b* represents the lipid moiety of our supported membrane.

To understand the limits for the nondestructive imaging of a supported membrane the following estimate might be helpful. Provided the lipid is in its crystalline state then the applied force from the tip would try to squeeze the tightly packed hydrocarbon chains which would eventually lead to a melting of the crystal. The difference in thickness between a crystalline and a fluid membrane is in the order of 10% (22). If we assume that the lipid assembly would tolerate a 10% deformation as an elastic load and above this limit it would melt, then one can estimate the mechanical work per molecule and compare it with the heat of melting known from calorimetry (23). The force which is needed to melt one molecule is then on the order of $F(\text{crit}) \approx 30\ \text{kJ}/(6.02 \times 10^{23} \times 0.2\ \text{nm}) \approx 0.3\ \text{nN}$. This value will be increased considerably by the cooperativity (>100 units) of the fluid-solid phase transition. Also due to a finite tip curvature the load will be distributed over several molecules. This again will reduce the effective force. This means that it is quite plausible that nondestructive imaging of solid membranes with forces <10 nN is possible.

Surface-induced polymerization of actin filaments

Actin, the most abundant protein in vertebrates, is one of the major components not only of the contractile elements of muscles but also of the cytoskeleton (11). This intracellular network of macromolecules maintains the shape and internal organization of cells and is also responsible for the motility of certain cells. It is obvious that for the motility a dynamical structural rearrangement of this network is required. The formation of certain structures like stress fibers appears to be restricted to the vicinity of the membrane, so that membrane properties might to some extent be involved in the underlying regulatory processes. This is one motivation to study the self-assembly of actin filaments at interfaces.

Under certain conditions actin self-assembles in vitro to form long filaments. We and others have shown that a self-assembly of actin filaments may occur in the vicinity of membranes under conditions where no polymerization occurs in the bulk phase, provided that these membranes are charged (23, 25). We have investigated this process using mica as a substrate because mica is known to carry

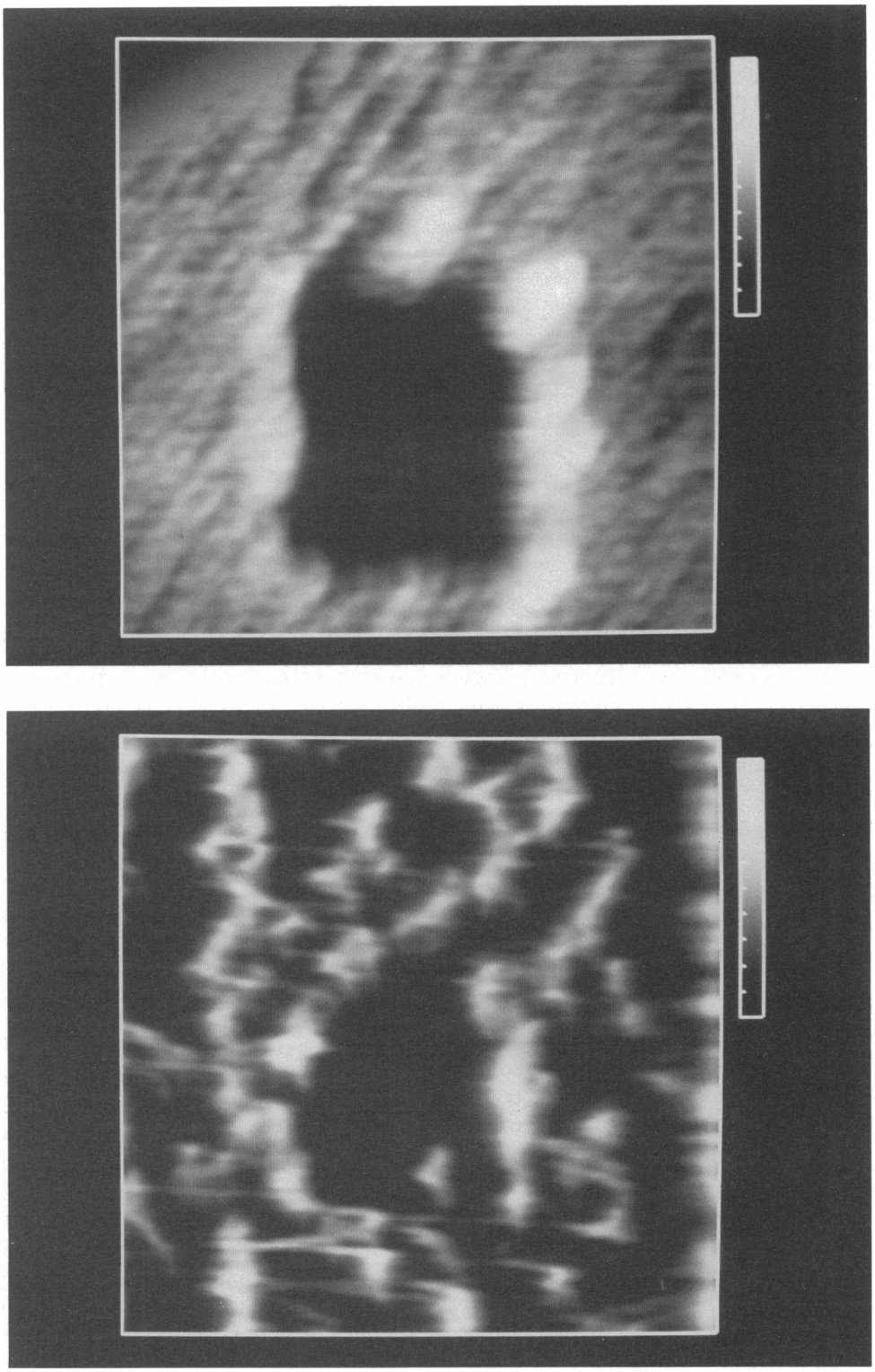

FIGURE 4 (*a*) Before this image of actin filaments on mica was taken the magnification was increased and the surface was scanned with a tip force of >30 nN for some frames. Then the area was reexamined at low force and decreased magnification again, which showed a flat square area with no actin in the middle of the picture. (image size: 748.0 nm, height: ~8.3 nm). (*b*) Same area as above but after 1M $CaCl_2$ was introduced and the surface has been incubated for ~5 min (image size: 748.0 nm, height: ~10.4 nm).

a surface charge density comparable to the negatively charged lipid membranes used in earlier studies (24).

Freshly cleaved mica was first imaged for calibrations purposes. Then a solution of 1 μg/ml actin in G-buffer was introduced. At scan rates of 40 lines per second (10 s per image) the formation of actin filaments at the surface was monitored. We did not observe the growth of individual filaments; they just appeared and the surface coverage became denser and denser. Fig. 3 *a* shows the surface ~5 min after incubation at low magnification. The surface is covered with thin filaments that in some cases exceed in length the field of view. Some of the filaments seem to cross over others. It is worth noting that the filaments are predominantly oriented perpendicular to the fast scanning direction. This was found to be true in several experiments of the same type. As long as the scanning force did not exceed 5 nN this image was found to be stable. Only minor rearrangements occurred. At a higher magnification individual filaments were scanned. The resulting image is given in Fig. 3 *b*. It shows blobs of ~5 nm in diameter arranged in a zigzag pattern. This structure is consistent with the generally accepted model of actin filaments (26) (see Fig. 3 *c*). Structural details of the filament are distinguishable. Only lowpass filtering was used in image processing. The surface-induced actin polymerization was also confirmed in a parallel experiment, where the filaments were imaged with Transmission Electron Microscopy (TEM) (see Fig. 3 *d*).

It is important to note that the actin layer which has formed at the surface is structured. So it is clearly not an adsorption process of monomeric actin molecules but a surface-induced polymerization process resulting finally in a dense surface layer of filaments. Whether or not this process plays any direct role in the structural reorganization of cytoskeletal networks cannot be deduced from these experiments, but these data show at least that there is a simple mechanism which could provide the formation of structures similar to those found in real cells. It is known that the formation of a seed of three monomeric subunits is the rate-limiting step for the actin polymerization (30). So it is highly probable that if there is an attractive interaction between the surface and actin, the actual concentration at the surface is increased and so the probability for the formation of a seed is increased. In addition the nucleation could also be promoted by the restricted mobility at the surface as well as orientational effects. This would be the simplest explanation of such a surface-driven polymerization.

To check the strength of the interaction of the actin filaments with the mica substrate the applied force was increased up to >30 nN in a smaller part of the field of view. By means of this it was possible to compare altered and unaltered areas in one scan by zooming out again at low applied force. The surface appeared as if the molecules would have been moved laterally and jammed into the surface layer of the unscanned areas (Fig. 4 *a*). A scan in the area where the molecules had been removed showed the typical structure of mica. It would be desirable to be able to quantitate the applied shear stress and compare it with known elastic properties of actin filaments (28) but unfortunately the curvature radius of the diamond tips are not known at present. Microfabricated cantilevers carrying integrated tips (these cantilevers and tips were developed by T. R. Albrecht and C. F. Quate and are now sold by Park Scientific Instruments, Mountain View, CA) will help to overcome this limitation. Thus future work may give quantitative information about mechanical properties of the filaments as well as about the interaction with various substrates.

From other experiments it is known that no such surface-induced polymerization occurs on membranes formed from neutral lipids such as lecithins (24, 25). It seems therefore likely that Coulomb interaction of actin with the charged mica surface is the major contribution to the effects shown above. To test for this hypothesis the ionic strength of the medium and thus the Debey length was altered. In a first step the ionic strength was drastically reduced by flushing with deionized water. In a bulk actin gel this leads to a depolymerization of the filaments, whereas in our case no disintegration of the filaments could be observed. An increase of the ionic strength, however, resulted in a degradation of the filaments (Fig. 4 *b*). Molecule clusters formed, which after some minutes disappeared from the surface, leaving behind a clean mica surface. We think that surface-induced polymerization of the actin filaments is promoted by a charge interaction of actin with the mica surface. This interaction could be shielded drastically by the high ionic strength which eventually led to a lift off from the surface.

CONCLUDING REMARKS

The AFM images of proteins in this report demonstrate clearly the enormous potential of this technique for the investigation of proteins in their functional environment. They also demonstrate the limits imposed by the AFM; the applied force involved in the imaging requires that the protein be immobilized at a solid surface. For Fab fragments this was accomplished by covalently binding to a lipid membrane. Proteins immobilized on lipid membranes can retain their functionality and still are restricted enough in their mobility to allow submolecular resolution using an AFM. Nevertheless an increase of the applied force to above 10 nN pushed aside the proteins; only the underlying membrane was then visible. The immobilization of the protein actin was accomplished with the much weaker Coulomb interaction to the surface

but was accompanied by a lateral polymerization. Again a force limitation for nondestructive imaging was found and convincingly demonstrated. This value is at the present very close to the technically practical minimal force. Advances in cantilever fabrication to allow lower forces together with the development of sample preparation techniques specifically for AFM studies will open up a wealth of applications in biology and medicine.

We would like to thank M. Bärmann for the actin; I. Sprenger, G. Keldermann, and T. Korda for technical support; J. Massie, P. Maivald, J. Gurley, and V. Elings of Digital Instruments for their generous support with advice, electronics, and software.

This research was also supported by an IBM Manufacturing Fellowship (A. L. Weisenhorn), the Office of Naval Research (B. Drake, C. B. Prater, P. K. Hansma), a National Science Foundation-Solid State Physics grant DMR89-17164 (S. A. Gould, P. K. Hansma), the Deutsche Forschungsgemeinschaft (M. Egger, H. E. Gaub), and the Volkswagen-Stiftung (S. P. Heyn, F. Ohnesorge).

Received for publication 13 March 1990 and in final form 11 July 1990.

REFERENCES

1. Binnig, G., C. F. Quate, and Ch. Gerber. 1986. Atomic force microscope. *Phys. Ref. Lett.* 56:930.
2. Binnig, G., Ch. Gerber, E. Stoll, T. R. Albrecht, and C. F. Quate. 1987. Atomic resolution with atomic force microscope. *Eur. Phys. Lett.* 3:1281.
3. Hansma, P. K., V. B. Elings, O. Marti, and C. E. Bracker. 1988. Scanning tunneling microscopy and atomic force microscopy: application to biology and technology. *Science (Wash. DC).* 242:209.
4. Drake, B., C. B. Prater, A. L. Weisenhorn, S. A. C. Gould, T. R. Albrecht, C. F. Quate, D. S. Cannell, H. G. Hansma, and P. K. Hansma. 1989. Imaging crystals, polymers and biological processes in water with atomic force microscope. *Science (Wash. DC).* 243:1586.
5. Deleted in proof
6. Balakrishnan, K., F. J. Hsu, D. G. Hafeman, and H. E. McConnell. 1982. Monoclonal antibodies to a nitroxide lipid hapten. *BBA.* 721:30–38
7. Egger, M., S. P. Heyn, and H. E. Gaub. 1990. Two-dimensional recognition pattern of lipid-anchored Fab' fragments. *Biophys. J.* 57:669–673.
8. Heyn, S. P., M. Egger, and H. E. Gaub. 1990. Lipid and lipid-protein monolayers spread from a vesicle suspension—a microfluorescence film balance study. *J. Phys. Chem.* 94/12:5073–5078.
9. Deleted in proof
10. Maoz, R., and J. Sagiv. 1984. On the formation and structure of self-assembling monolayers. *J. Colloid Interface Sci.* 100:465–496.
11. Spudich, J. A., and S. Watts. 1971. The regulation of rabbit skeletal muscle contraction. 1. Biochemical studies of the interaction of the tropomyosin/troponin complex with actin and the proteolytic fragments of myosin. *J. Biol. Chem.* 246:4866–4871.
12. MacLean-Fletcher, S. D., and T. D. Pollard. 1980. Identification of a factor in conventional muscle actin preparations which inhibits actin filament self-association. *Biochem. Biophys. Res. Commun.* 96:18–27.
13. Alexander S., L. Hellemans, O. Marti, J. Schneir, V. Elings, P. K. Hansma, M. Longmire, and J. Gurley. 1989. An atomic-resolution atomic-force microscope implemented using an optical lever. *J. Appl. Phys.* 65:164.
14. Amer, N. M., and G. Meyer. 1988. A simple optical method for a remote sensing of stylus delection in atomic force microscopy. *Bull. Am. Phys. Soc.* 33:319.
15. Meyer, G., and N. M. Amer. 1988. Novel approach to atomic force microscopy. *Appl. Phys. Lett.* 53:2400.
16. Albrecht, T. R., and C. F. Quate. 1988. Atomic resolution with an atomic force microscope on conductors and nonconductors. *J. Vac. Sci. Technol.* A6:271.
17. McConnell, H. M., T. H. Watts, R. M. Weis, and A. A. Brian. 1986. Supported planar membranes. *B.B.A. (Biochim. Biophys. Acta) Libr.* 864:95–106.
18. Watts, T. H., H. E. Gaub, and H. M. McConnell. 1986. T-cell-mediated association of peptide antigen and major histocompatibility complex protein detected by energy transfer in an evanescent wave-field. *Nature (Lond.).* 320:179–181.
19. Davis, D. R., E. A. Padlan, and D. M. Segal. 1975. Three-dimensional structure of immunoglobins. *Annu. Rev. Biochem.* 44:639.
20. Gould, S. A. C., B. Drake, C. B. Prater, A. L. Weisenhorn, S. Manne, H. G. Hansma, P. K. Hansma, J. Masse, M. Longmire, V. Elings, B. Dixon Northern, B. Mukergee, C. M. Peterson, W. Stoeckenius, T. R. Albrecht, and C. F. Quate. 1990. From atoms to integrated circuit chips, blood cells and bacteria with the atomic force microscope. *J. Vac. Sci. Technol.* A8:369–373.
21. Merkel, R., E. Sackmann, and E. Evans. 1989. Molecular friction and epitactic coupling between monolayers in supported bilayers. *J. Phys. France.* 50:1535–1555.
22. Büldt, G., H. U. Gally, A. Seelig, and J. Seelig. 1978. Neutron Diffraction Studies on Selectively Deuterated Phospholipid Bilayers. *Nature (Lond.).* 271:182–184.
23. Jürgens, E., G. Höhne, and E. Sackmann. 1983. Calorimetric study of the dipalmitoylphosphatidylcholin/water phase diagram. *Ber. Bunsen-ges. Phys. Chem.* 87:95–104.
24. Zimmermann, R., Ch.F. Schmidt, M. Bärmann, G. Isenberg, and H. E. Gaub. 1990. Polymerization of actin on supported lipid bilayers. *In* Cytoskeletal and Extracellular Proteins, Structure, Intractions and Assembly. U. Aebi and J. Engel, editors. Springer Verlag, Heidelberg, Berlin, New York. Series in Biophysics Vol. III Section IV 233–234.
25. Laliberte, A., and C. Gicquaud. 1988. Polymerization of actin by positively charged liposomes. *J. Cell Biol.* 6:1221–1227.
26. Korn, E. D. 1982. Actin Polymerization and its Regulation by Proteins from Nonmuscle Cells. *Physiol. Rev.* 62:672–737.
27. Gaertner, A., K. Ruhnau, E. Schröer, N. Selve, M. Wanger, and A. Wegner. 1989. Probing Nucleation, Cutting and Capping of Actin Filaments. *J. Muscle Res. Cell Motil.* 10:1–9.
28. Schmidt, Ch.F., M. Bärmann, G. Isenberg, and E. Sackmann. 1989. Chain dynamics, mesh size and diffusive transport in networks of polymerized actin. A quasielastic light scattering and microfluorescence study. *Macromol.* 22:3638–3649.
29. Neugebauer, D.-Ch., and H. P. Zingsheim. 1979. Apparent holes in rotary shadowed proteins: dependence on angle of shadowing and replika thickness. *J. Microscopy* 117:313–315.